TRIBOLOGICAL CHARACTERIZATION OF VARIOUS LUBRICIN-MIMETIC POLYMERS FOR BIOLUBRICATION APPLICATIONS

A Thesis

Presented to the Faculty of the Graduate School

of Cornell University

In Partial Fulfillment of the Requirements for the Degree of

Master of Science

by

Ya Guan

August 2017

BIOGRAPHICAL SKETCH

Ya completed his undergraduate studies in the Polymer Science and Engineering department at Zhejiang University, China in July 2015. He began researching synthetic polymers for biolubrication applications in Dr. Delphine Gourdon's laboratory in the fall of 2015 for his M.S. at Cornell. After completing his master's degree, Ya will enter the Ph.D. program in Materials Science and Engineering at The Ohio State University.

ABSTRACT

Healthy articular joints exhibit highly efficient lubrication and wear resistance. However, joints do not heal easily after injury and they are subjected to severe diseases, such as osteoarthritis (OA). Lubricin, an important component of synovial fluid, is recognized to have a major lubricating role in cartilage. The loss of lubricin is considered to be a factor in the pathology of OA. Lubricin has a bottle-brush architecture, which provides excellent lubrication because it prevents interpenetration between brushes bound to shearing surfaces. Inspired by this bottle-brush structure, a series of lubricin-mimetic polymers (mimLUBs) has been synthesized by the Putnam Group at Cornell.

In this study, we used the Surface Forces Apparatus (SFA) to characterize the tribological properties of three different types of synthetic mimLUBs. All polymers shared the same lubricating domain but possessed binding units either (i) at one terminus (ii) at both termini or (iii) randomly distributed throughout their backbone. First, SFA compressive normal force measurements were performed on mimLUB-coated mica surfaces to assess both the uncompressed film thickness and the ability of each mimetic to resist to compression without being squeezed out of the junction. Second, the SFA was used to monitor both the friction forces and the onset of damage between sheared mimLUB-coated mica surfaces. Our data indicate that the two mimLUB polymers with binding units located either at one terminus or at both termini could achieve friction coefficients below the friction coefficient of lubricin sheared between mica surfaces, while the polymer with randomly distributed binding units failed to lubricate. Overall, two out of the three mimLUBs tested had good lubricating

and wear protecting abilities, at relatively high shearing velocities and pressures.

Collectively, our findings suggest that, by tuning their molecular structure, engineered lubricin-mimetics can achieve good binding affinity and lubricating ability.

ACKNOWLEDGMENTS

Firstly, I would like to thank Prof. Gourdon for her kind guidance to my scientific research and life throughout two years. 2-year master research in U.S. is challenging to me at the beginning and I feel lucky to have her as my advisor. I also want to thank Prof. Putnam and his Ph.D. student Zhexun Sun for providing me with not only the polymer, but a lot of useful advice. I would like to thank Sierra Cook for teaching me the experimental skills, data analysis and interpretation since the first day I joined the group. SFA is a very complex device and I could not carry out the research without her help. Noah Pacifici, Evan Czako, Annie Fang, Adeline Tse and Kate Lerigoleur participated in mica cleaving, silvering and data analysis. I appreciate their help. Last but not the least, I would like to thank my parents and all my friends.

TABLE OF CONTENTS

CHAPTER 1

DESIGN OF LUBRICIN-MIMETIC POLYMERS

1.1 Background

1.1.1 Articular joints, synovial fluid and lubricin

In the human body, healthy articular joints exhibit highly efficient lubrication and wear resistance. Though the pressure applied on cartilage surfaces can be up to 18 MPa, wear usually does not happen in the articular joints of a healthy person throughout the entire life[1]. However, injuries on articular joints can lead to debilitating diseases and it is difficult to self-heal. Osteoarthritis(OA) is one of the most common and fast growing diseases in the world. It can not be cured and can result in disability. OA is often related with increasing wear in the cartilage (Figure 1.1). The etiology of OA remains unknown and treatment has limited help[2]. There are more than 3 million cases per year in US and it affects more than 40 million individuals[3].

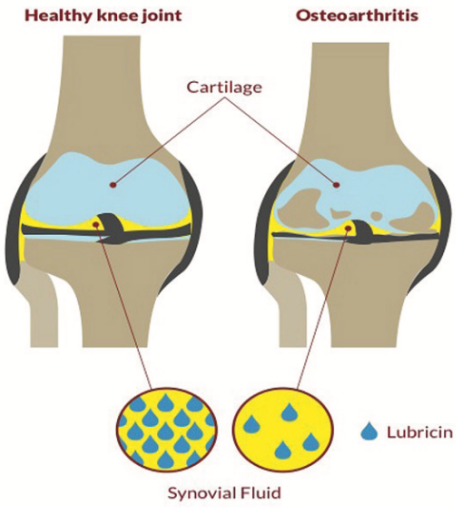

Figure 1.1 Healthy knee joint and joint with osteoarthritis in human body[4]

It has been reported that in OA patients, a volume of the major joint lubricant called synovial fluid is depleted compared to healthy joints (Figure 1.1)[4]. There are various components in synovial fluid which interact synergistically to lubricate the cartilage[5]. Lubricin is a synovial fluid component which is known to contribute to the extremely low boundary ode friction coefficients in healthy joints. In OA patients, the amount of lubricin in the synovial fluid is also depleted.[6].

1.1.2 Molecular structure of lubricin

Due to the critical role that lubricin plays in joint lubrication, plus the relation between lubricin deficit and the pathology of OA, there is a strong motivation to find alternatives to lubricin that are able to help lubricate the cartilage surface and prevent wear. Consequently, the development of a viable, affordable synthetic to lubricin of great scientific and clinical relevance.

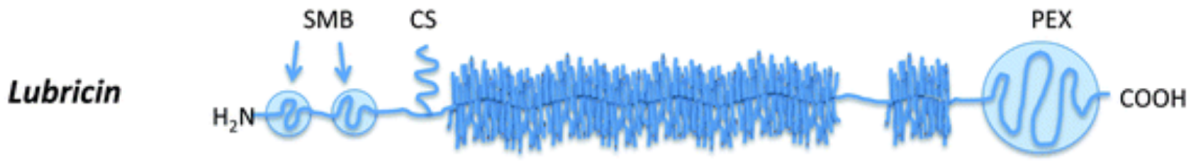

Figure 1.2 Schematic of the molecular structure of lubricin[7]

Lubricin has three distinct domains. A typical lubricin molecule has a long mucin-like glycoprotein domain in the middle, a hemopexin (PEX) domain at the C-terminus and a somatomedin (SMB) domain at the N-terminus[8]. The mucin-like domain consists of a poly-peptide backbone and is hydrophilic. It has a bottle-brush structure as shown in Figure 1.2. The hydrophilic bottle-brush structure is crucial in lubrication because with the water bound to the molecules, they can slide past each other instead of

interpenetrating into each other which would cause significantly higher friction. This mechanism is similar to the lubrication of polyelectrolytes[9]. It is has been reported that lubricin uses its C-terminus to bind to cartilage[10] and N-terminus to form a dimer with the thiol group in this domain. Therefore, lubricin is considered to adopt an loop-like architecture on cartilage surface[11]. The strong attachment of lubricin to the cartilage surface is also important in lubrication because higher load, pressure, or sliding speed would remove weakly-attached lubricants and increase the friction and wear

1.1.3 Previous study on lubricin-mimetic

Inspired by the molecular structure of lubricin, two key factors for a good mimLUB are proposed: hydrophilic bottle-brush architecture and strong attachment to the surface. A lot of work has been done to synthesize mimLUB and characterize its tribological properties.

Banquy et al designed an "ABA" triblock copolymer to mimic lubricin (Figure 1.3)[12.] They used a zwitterionic polymer poly 2-methacryloyloxyethyl phosphorylcholine (PMPC) to mimic the bottle-brush structure. PMPC is considered to be a biocompatible polymer because it resists nonspecific protein absorption very well. As shown in panel C, this mimLUB has a hydrophilic, zwitterionic lubricating domain and a positively charged quaternary amine binding domain which is used to bind to the negative surface in their system.

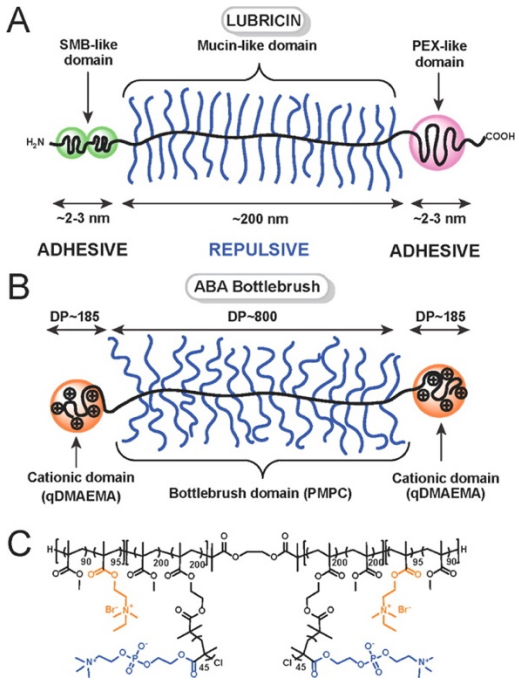

Figure 1.3 Schematics of LUB and a zwitterionic bottle-brush polymer mimicking LUB[12].

As for lubrication, this zwitterionic ABA mimLUB has a lower friction coefficient ($\mu = 0.015$) than lubricin ($\mu = 0.038$) under the same condition (shearing medium, sliding speed, concentration, etc.), exhibiting a good lubricating ability. They also sheared the mimLUB in water and found an even lower friction coefficient due to a more extended conformation in water compared to PBS.

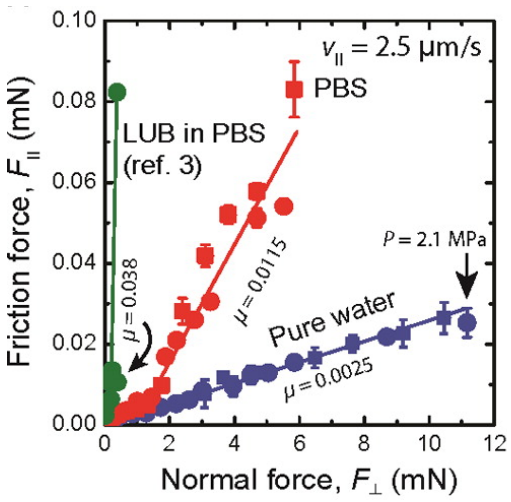

Figure 1.4 Friction data of zwitterionic ABA mimLUB[12].

Another example of recent research focused on developing and characterizing lubricin mimetics is a collaboration between the Putnam and Gourdon groups at Cornell University. The Putnam group designed a mimLUB with poly acrylic-acid (PAA) as the backbone and poly ethylene-glycol (PEG) grafted on the side chains as the lubricating domain[13]. PEG is another well-studied biocompatible and hydrophilic polymer and is suitable for the bottle-brush architecture. A single thiol-terminated binding group was designed to bind to the gold surface which they used to carry on the friction characterization. Our group also used the SFA device to characterize its lubricating ability[14]. It turned out that the friction coefficient is high and damage occurred at an early stage.

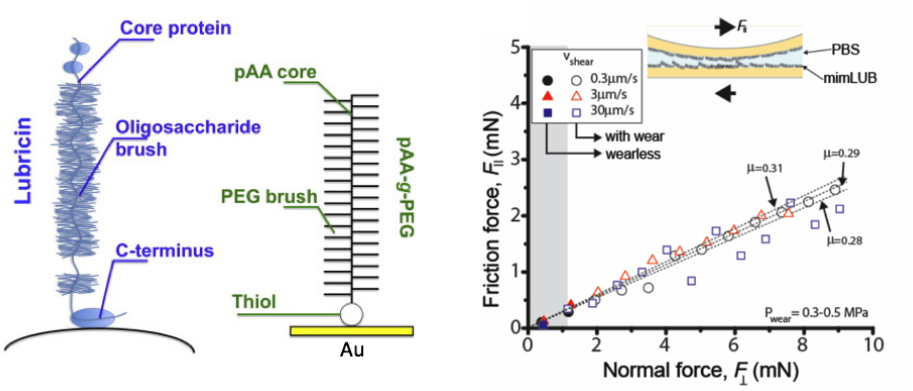

Figure 1.5 Molecular structure and friction data of a PAA-g-PEG mimLUB[13 15]

Tribological characterization performed by our group requires that the mimLUB under study is incubated between two negatively-charged surfaces (see details in Chapter 2). The binding group in this design is thiol group, which does not tend to bind well to the negative surface.

1.2 Design of a new series of lubricin-mimetic polymers

A new design for a PAA-PEG mimLUBwas proposed by Zhexun Sun from Putnam's group (Figure 1.6, Figure 1.7(left)).

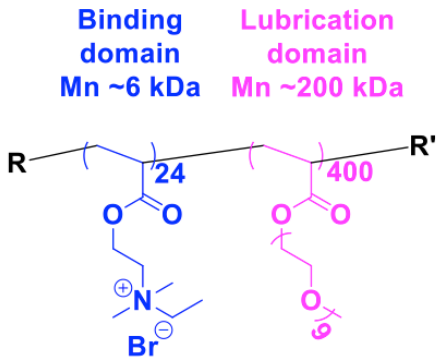

Figure 1.6 Molecular structure of AB diblock lubricin-mimetic polymer

It is a diblock copolymer named ‘AB’. ‘A’ is the binding domain with 24 repeating units of PAA backbone with quaternary amine group while B is the lubricating domain with 400 repeating units of PAA backbone with PEG grafted on the side chains. The positively charged part is responsible for binding to the surface while the PEG part is to mimic the bottle brush domain of lubricin.

In the schematic shown in Figure 1.7 (left), the red dots represent the backbone with binding groups whereas the bottle-brush represent the lubricating domain. To better understand the function of binding domain and lubricating domain and the relationship between molecular structure and lubricating ability, they designed another two types of mimLUBs.

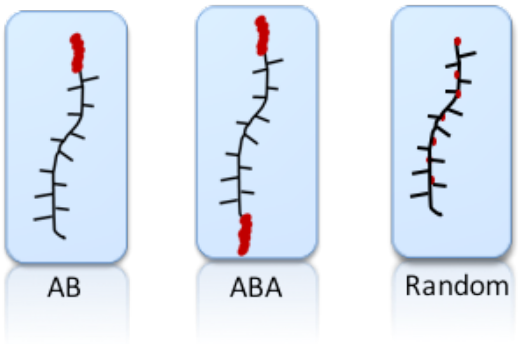

Figure 1.7 Schematics of three types of lubricin-mimetic polymers (red dots: binding domain, bottle-brush: lubricating domain)

One is called ABA (Figure 1.7 (middle)). The only difference compared with AB is that ABA has another 24 repeat units of the acrylic acid backbone with quaternary amine binding groups on the other side of the molecule. ABA has binding domain at both ends and is expected to bind to the surface easily. The other design is called

Random (Figure 1.7 (right)). The binding groups of Random mimLUB are distributed randomly on the backbones.

The molecular weight of three types of mimLUBs are similar (~200kDa) since it is dominated by the lubricating domain which consists of 400 repeat units for all three types of polymers.

Polymer	Hydrodynamic size (nm)
AB	25
ABA	25
Random	19

Table 1.1 Hydrodynamic size of three types of mimLUBs

Table 1.1 shows the hydrodynamic size of AB, ABA and Random mimLUBs measured via dynamic light scattering. We note that the size of Random is smaller than the other two while ABA and AB have the same size. One possible explanation is that the quaternary amine binding groups gather together in AB and ABA. The repulsive force among the positively charged groups makes the molecule larger than Random mimLUB where the binding groups are distributed sparsely.

1.3 Motivation and goal

The goal of this project is to characterize the lubricating ability of three types of mimLUBs to determine whether they are potential alternatives to lubricin. We proposed three criterions for a good lubricant: strong attachment to the surface, low friction coefficient (compared with lubricin under the same condition) and good wear

protecting ability. All three characterizations can be carried out via Surface Force Apparatus (see Chapter 2).

In addition, we hypothesized that there is connection between molecular structure, conformation on the surface, and lubrication. By characterizing three different types of mimLUBs that have different molecular structures, we want to figure out the correlation.

CHAPTER 2

TRIBOLOGICAL STUDY OF LUBRICIN-MIMETIC POLYMERS

2.1 Background and motivation

2.1.1 Lubrication in physiological environment

Lubrication is a critical issue in the industrial revolution since it reduces energy cost and increases the lifetime of various machines. Lubrication is also very important in human body because daily exercise (e.g. walking, running, jumping etc.) causes a lot of stress and pressure on the joints. Lubrication can minimize the wear and prevent us from some severe diseases. We differentiate two modes of lubrication based on the lubrication regimes: hydrodynamic lubrication and boundary lubrication.

When cartilages surfaces are separated from each other, the synovial fluid provides hydrodynamic lubrication[1]. In this mode, the friction is determined by the viscosity of the fluid in the junction, as well as the sliding speed, load and pressure. Synovial fluid is extremely viscous so that the friction coefficient in this regime is very low. At low shearing velocities and under higher loads, the hydrodynamic lubrication breaks down since the viscous, lubricating film is squeezed out. If all the synovial fluid components are removed, the friction coefficient would be very high since dry friction happens in this case. However, in the real case, a thin polymer layer was found to remain absorbed on the cartilage surface, making the friction much lower than dry friction. The major glycoprotein in this thin layer was first purified by Radin et al. [16] and they named it lubricin[17]. The polymer layer might also contain HA and phospholipids. Such

lubrication where a layer of polymer remains adsorbed at direct cartilage-cartilage contact is so-called boundary lubrication.

In boundary lubrication mode, lubricin helps reduce the friciton between the cartilage surfaces. It is discovered that a lubricating film of only one layer of molecules is sufficient to achieve a good lubrication[18].

Figure 2.1 shows the friction coefficient of different lubrication modes. Hydrodynamic lubrication produces a friction coefficient which depends on viscosity, speed and load whereas boundary lubrication has a high friction regardless of these parameters. In reality, we often encounter a combination of hydrodynamic lubrication and boundary lubrication. Because lubricin is known to be a good boundary lubricant, we focus on characterizing the lubrication of mimLUB in the boundary lubricating regime.

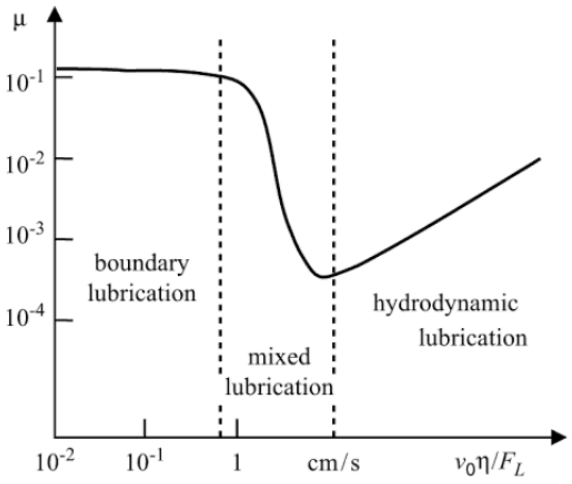

Figure 2.1 Three regimes of lubrication and the friction coefficient plot versus sliding speed, viscosity and load[19]

2.1.2 Lubrication of lubricin on mica surfaces

Mica is chosen to model negatively charged lipids and glycoproteins found in cartilage because mica is also negatively charged. In addition, friction tests require very high accuracy. Using mica can exclude the friction generated by surface itself because mica is flat and atomically smooth (roughness <0.1 mm). Both lubricin and synthetic lubricin-mimetic polymers have a positively charged binding group, which can bind with mica very well. A key difference between cartilage and mica is that cartilage tissue is porous whereas mica is non-porous. Using a non-porous surface allows precise isolated measurements of the friction and interactions occurring in the confined film between the mica surfaces without the complicating factors that are introduced when the confined film can penetrate into the confining surface. Therefore, mica is an ideal model to study lubrication at the molecular scale.

The lubrication of lubricin on mica surface is well studied[20]. The friction force versus normal load of shearing lubricin between two mica surfaces in PBS is shown in Figure 2.2.

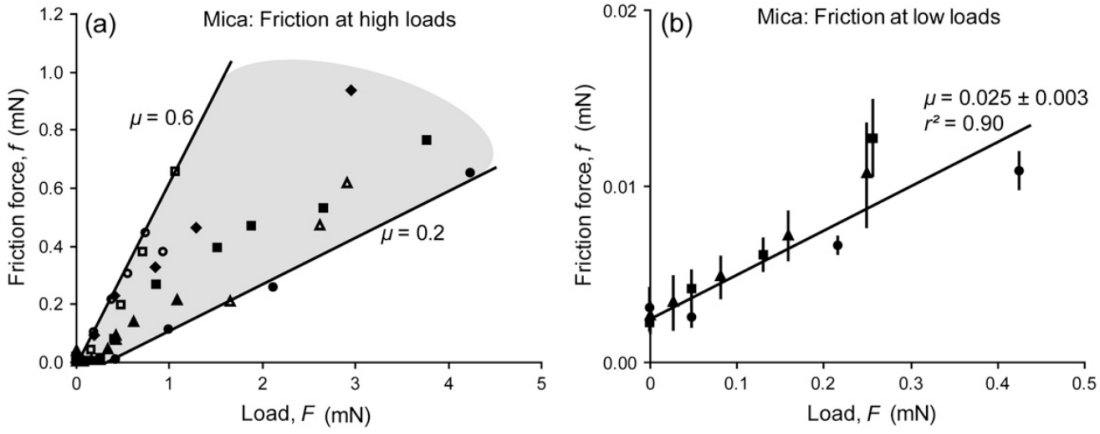

Figure 2.2 Friction coefficient of shearing lubricin between two mica surfaces in PBS at low(left) and high(right) loads[20]

At high loads (F > 0.5 mN) the friction coefficient measurements are quite scattered but all fall into the range of 0.2-0.6, whereas at low loads (F <0.5 mN) the measurements are highly consistent at $\mu = 0.025$. For SFA tribological measurement in our study, the load is always greater than 0.5. Therefore, it is appropriate to compare the friction coefficient measured for mimLUB polymers with that of lubricin at high loads (i.e. F > 0.5 mN).

2.2 Materials and Methods

2.2.1 Mica cleaving, silvering and preparation of surfaces.

Figure 2.3 shows the general procedure of how surfaces are prepared for experiments. A large, step-free sheet of mica (S&J Trading, Glen Oaks, NY, USA) was selected as a backing sheet. Then thinner and smaller sheets (2-4 μm thick) were cleaved as the substrate surfaces in experiments and put onto the backing sheet with the clean side facing down. The size of the mica piece should be large enough to cover the area of two 1cm silica discs. The color of these mica sheets should be uniform to ensure the homogeneity. A hot platinum wire cutter (0.2 mm) connected to a low voltage DC power supply was used to trim the edge of the thin mica sheet to make it easier to peel off. The voltage is set to be around 2-2.5 V and the platinum wire should look bright orange. All these operations should be done in a laminar flow dust-free cabinet in case mica flakes fall onto freshly cleaved mica pieces. An air blower is used to get rid of the mica flakes created when we are cleaving.

Mica is transparent. It should be coated with some highly reflective layer on the back to reflect the light back and forth to create an interferometer. Silver is an ideal coating material.

The backing sheets were silvered in a vacuum coating unit (Varian Bell Jar Thermal Evaporator) at a pressure of 2×10^{-6} Torr. Silver was put onto a molybdenum boat connected in a circuit to generate heat. Silver was deposited at a rate of ~1 Å/sec to form a uniform layer of 550 Å. The mica backing sheet should be far away from the molybdenum boat to prevent overheating.

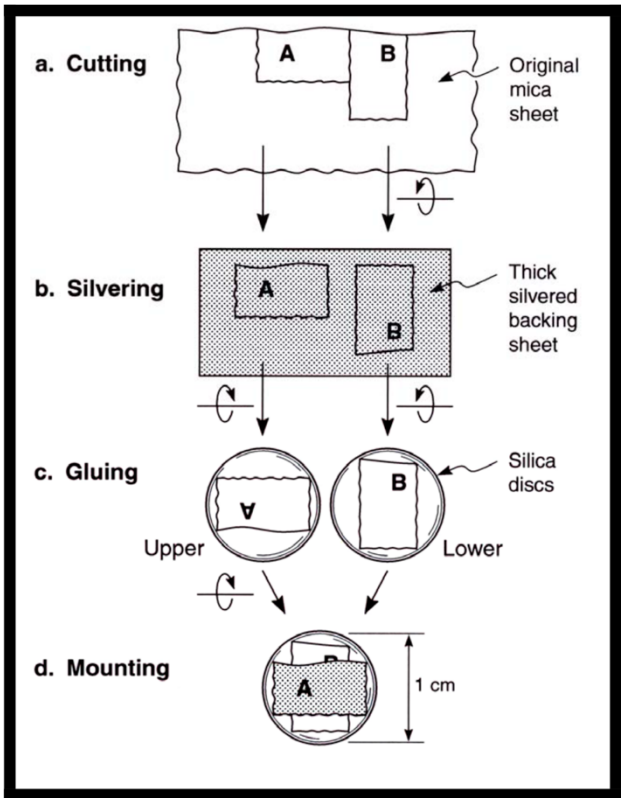

Figure 2.3 Preparation of surfaces coated with back-silvered mica[21]

After cleaving and silvering, the backing sheet should be kept in a desiccator for later use to avoid oxidation.

Back silvered mica sections were glued onto half cylindrical silica discs with UV curing glue (Norland, Cranbury, NJ, USA). After gluing the mica sheets, they are cured by UV irradiation for 4 h. To remove the glued mica, we put it in chloroform overnight then peel off mica sheets, clean it with methanol and store it for later use.

2.2.2. Surface Force Apparatus

2.2.2.1 Basic optics

Interference and Newton's ring

The Surface Forces Apparatus (SFA) was developed in the 1970s by Jacob Israelachvilli. It measures normal forces with 10 nN precision while simultaneously measuring surface separation with 1nm resolution in real time. With the help of the friction device, it can also precisely measure the coefficient of friction. Last but not the least, surface damage can be detected by monitoring the fringes of equal chromatic order (FECO).

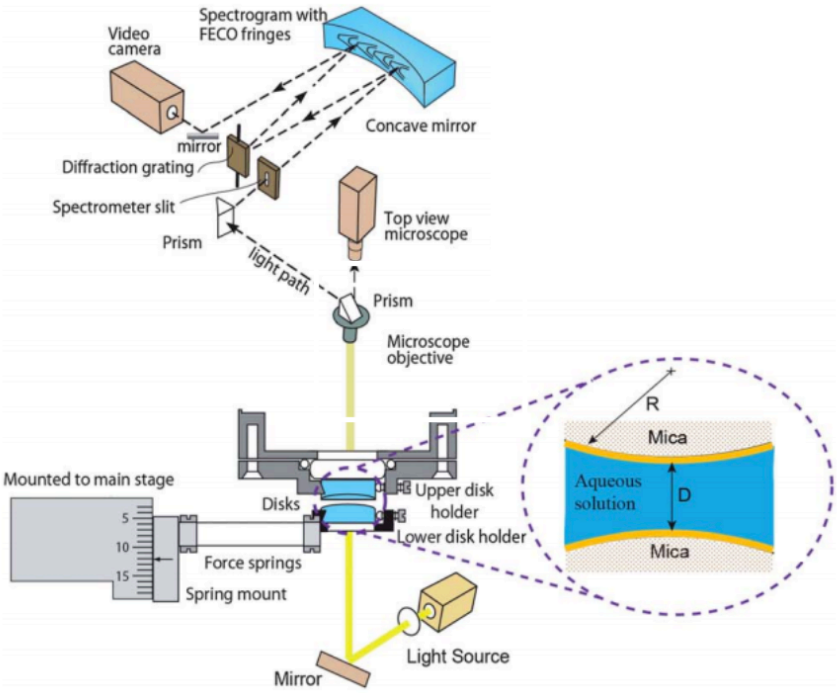

Figure 2.4 General optics in the surface force apparatus[21]

As shown in Figure 2.4, the material under study, which in our case was the polymer solution, was put in between two cross-configured semi-cylindrical mica surfaces. White light shone through the surfaces. Since the surfaces were covered with back-silvered mica, the light was reflected back and forth by the silver layer, creating lights with different phases which resulted in interference. This system can be treated as an optical interferometer (Figure 2.5).

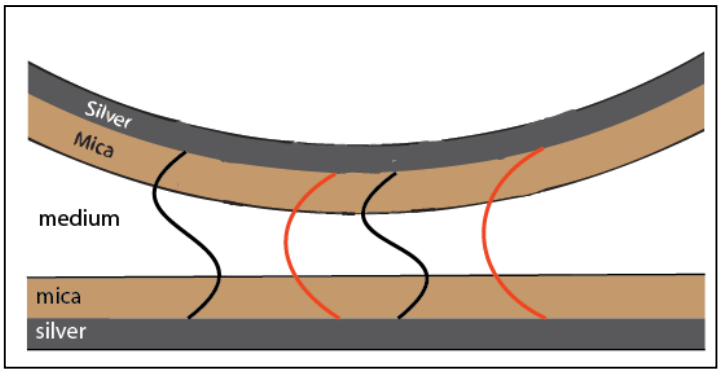

Figure 2.5 The material under study is put in between cross-configured cylindrical silica surfaces coated in back-silvered mica, creating an optical interferometer

The condition for constructive interference requires that wavelengths must fit into gap (2D) an integer multiple of times

$$n\lambda = 2D \tag{2.1}$$

Based on equation (2.1), we can determine the separation distance by measuring the wavelength of the interference fringes. As we separate surfaces (D increases), higher wavelengths exist in the interferometer.

Since the surfaces are in a cross-configured cylindrical configuration (Figure 2.6 left), it has the same geometry as a sphere on a flat surface. Therefore, when the surfaces are very close, we can observe the Newton's ring (Figure 2.6 right), which is caused by constructive interference. We can view this pattern through a microscope.

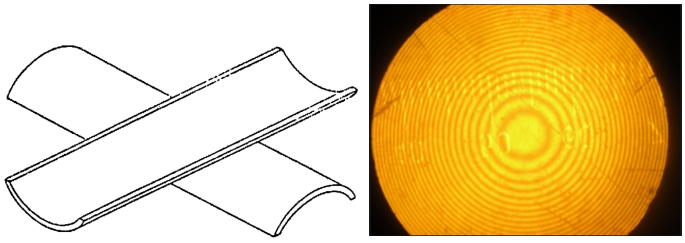

Figure 2.6 (left) Cross-configured cylindrical configuration (right) Newton's Ring[22]

The transmitted light consists of a set of discrete wavelengths, which can be observed as fringes by passing Newton's rings through an ordinary grating spectrometer. Such fringes are so-called fringes of equal chromatic order (FECO).

Even fringes have maximum wave amplitude and it is affected by the index of refraction of the material whereas odd fringes have minimum amplitude and is not affected by the index of refraction.

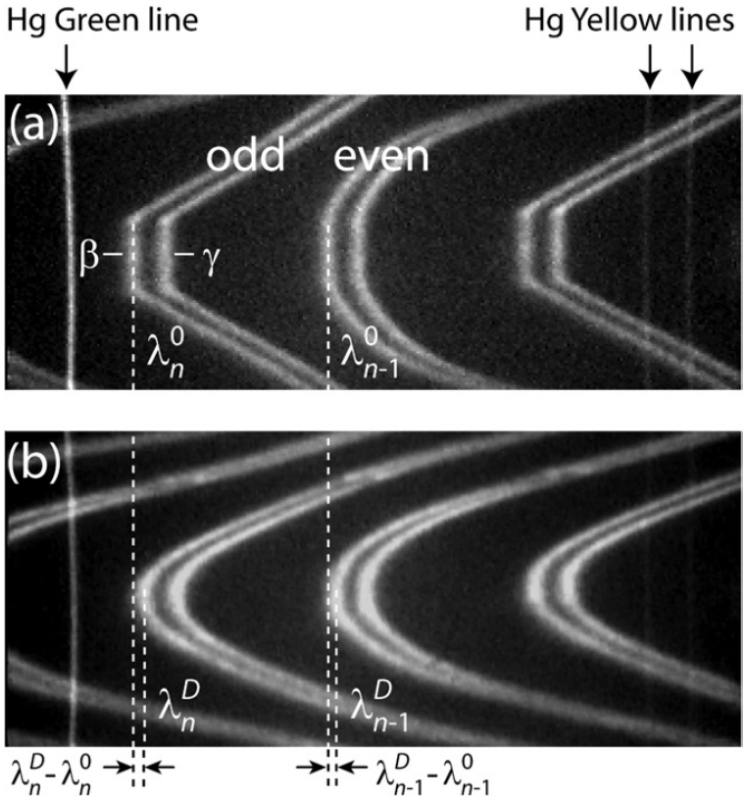

Figure 2.7 Sample FECO images: vertical lines are the mercury lines used to calibrate the wavelength[23]

Odd order fringes and even order fringes have different shapes (Figure 2.7). Each fringe contains a β-component and a γ-component. This doublet pattern is due to the birefringence of mica. The vertical lines in the picture are mercury lines (green and yellow) used to calibrate the wavelengths.

When the surfaces are in contact with nothing else in the junction, the interference fringes depend on the mica thickness. In our experiment setting, it is better to have

fewer fringes (i.e. thinner mica) because the resolution is higher with fewer fringes. When the surfaces are brought apart, fringes move to higher wavelengths (to the right). The separation distance, *D*, can be determined by measuring the corresponding wavelengths and comparing with mica-mica contact where $D = 0$. The equation is given as follow

$$D = \frac{n F_n (\lambda_n^D - \lambda_n^0)}{2\mu_{mica}} \qquad (2.2)$$

where μ is the index of refraction of mica.

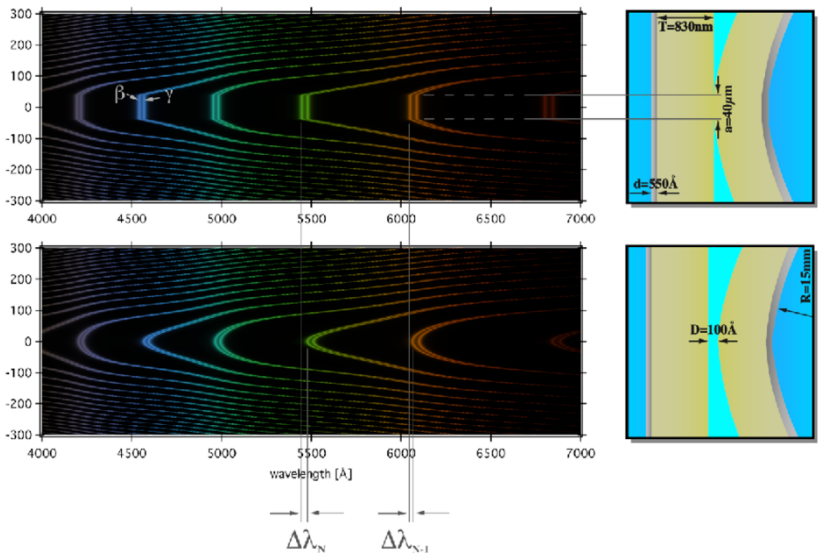

Figure 2.8 FECO images showing (a) surfaces that are in contact and (b) surfaces that are brought apart.[21]

FECO can provide us with the most important information. Apart from the separation distance, we also know the contact shape, diameter, the existence of some particle build-ups and damage since the shape of the fringes directly corresponds to the shape

of the surfaces.

It is notable that when damage happens, the discontinuity is always visible on both fringes. If it is only visible on the even fringe, it is probably just a change in the index of refraction of the material.

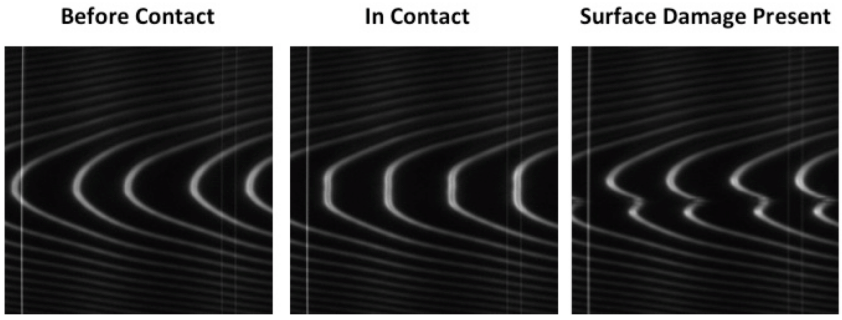

Figure 2.9 FECO images when surfaces are before contact (left), in contact (middle) and damaged (right).

In addition, there is a difference between mica/surface damage and polymer film damage. When the polymer film is damaged, the fringes often deform a little bit. However, when mica surface is damaged, we often observe discontinuous fringes as shown in Figure 2.9 (right).

2.2.2.2 Normal force measurement

Figure 2.10 shows the basic parts in the SFA

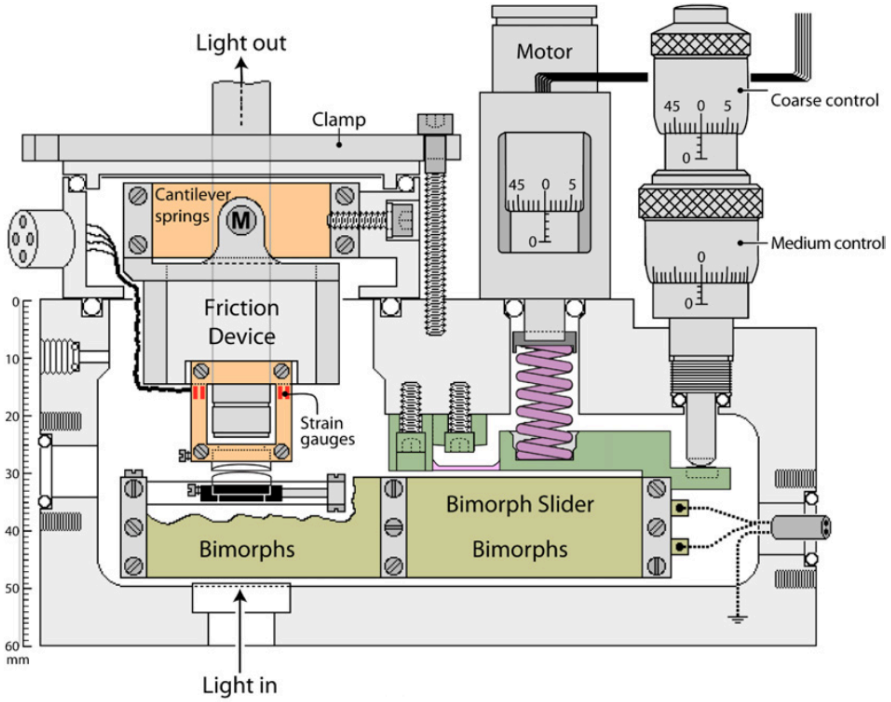

Figure 2.10 Mechanics under the surface force apparatus[23]

The bottom surface is mounted on a cantilever spring. When force is applied, the spring buckles following Hooke's Law. There are three ways to to move the bottom surface in order to control the separation distance between two surfaces: (1) the coarse differential micrometer that can move the surface up to 2 mm; (2) the medium differential micrometer that can move the surface up to 200 μm; (3) the fine control that can move up to 10 μm using a motor which drives a fine micrometer with a very high accuracy of 2 Å. Even more accurate distance control can be achieved by moving the upper surface with a piezoelectric mount, which will be discussed in the next chapter.

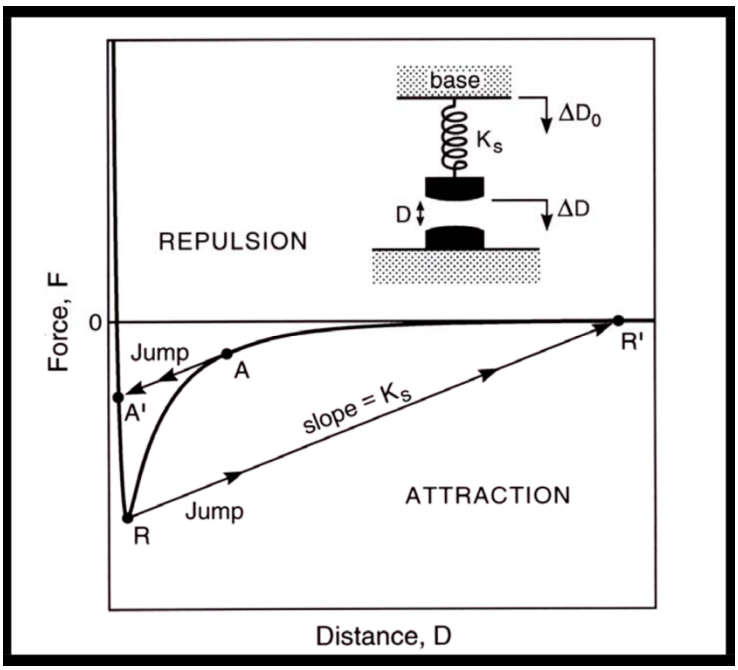

Figure 2.11. Basic mechanics of the force measuring system[21]

Difference between displacement of the motor ΔD_0 and the displacement of the surface ΔD yields the spring deflection (Figure 2.11). From the spring deflection, one can calculate the force using Hooke's law.

$$F = -K_s (\Delta D_0 - \Delta D) \tag{2.3}$$

When we run an experiment we move the motor continuously, and since the the motor is moving at a constant speed, we can get the displacement of the motor as a function of time. We can also extract the actual position of the surface from the FECO fringes as a function of time.

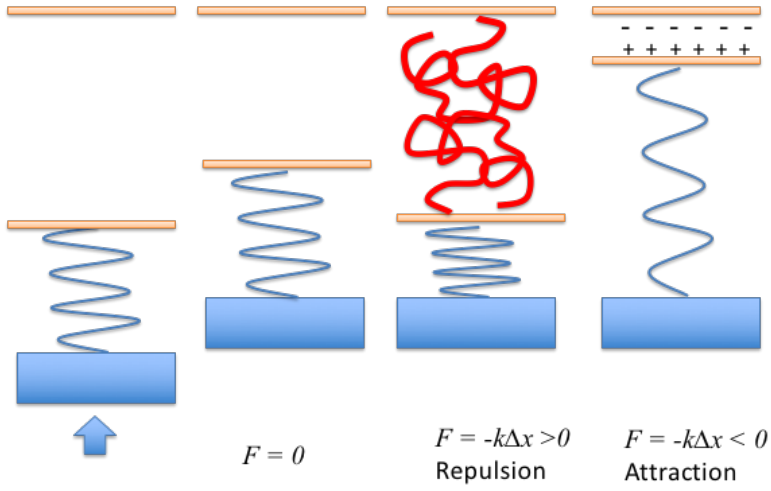

Figure 2.12 Schematics showing the principle of normal force measurement

As shown in Figure 2.12, when there is nothing between two surfaces, the actual distance should follow the linear relationship (i.e. $\Delta D_0 = \Delta D$). Any deviation from the linear function is caused by either adhesive force or repulsive force. If there are polymers between two surfaces, once the surfaces are brought close enough such that the polymers on both sides interact with each other, the actual movement of the surfaces will be smaller the the displacement of the motor. In this case the spring is compressed (i.e. $\Delta x > 0$), creating a negative, repulsive force. If there is an attractive force between two surfaces (e.g. adhesion, electrostatic force, magnetic force), the spring is stretched, creating a positive force.

We often measure forces both on approach (inward run) and separation (outward run). On approach, the surfaces are moved closer at a constant rate, from which we can derive the linear relationship between position and time. The position where the repulsive force appears is often called the onset of interaction D_0. At a very large load,

the interaction of polymers reaches an equilibrium and the distance does not change with time. The final distance is so-called “hard wall” thickness (HW).

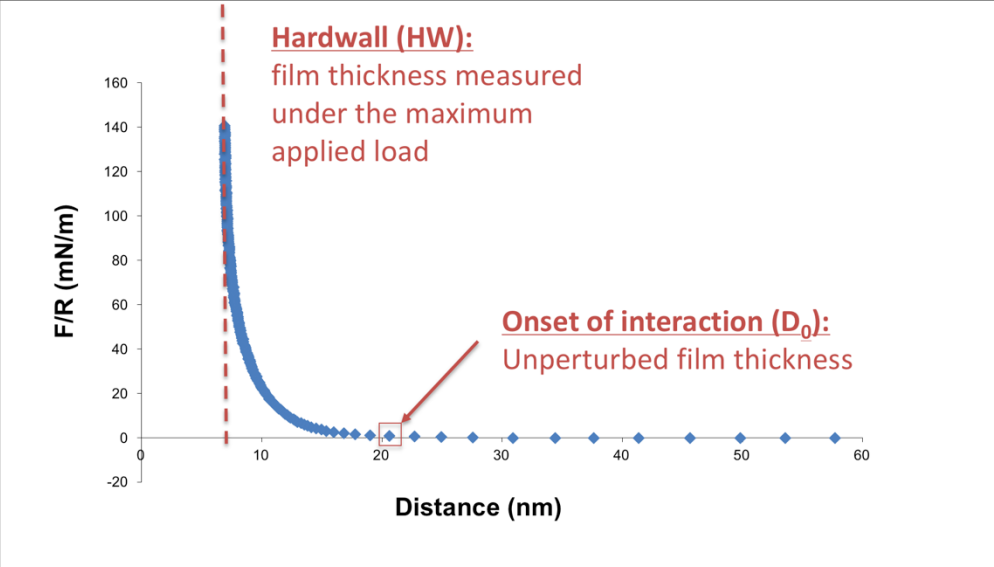

Figure 2.13 A sample normal force run with onset of interaction and hardwall

The SFA can be mounted with various cantilever springs ranging several orders of magnitude in stiffness.The procedure for calibratingthe springs used in our experiments can be found in the Appendix.

2.2.2.3 Friction measurement

Figure 2.14 illustrates the basic principles of the friction measurement.

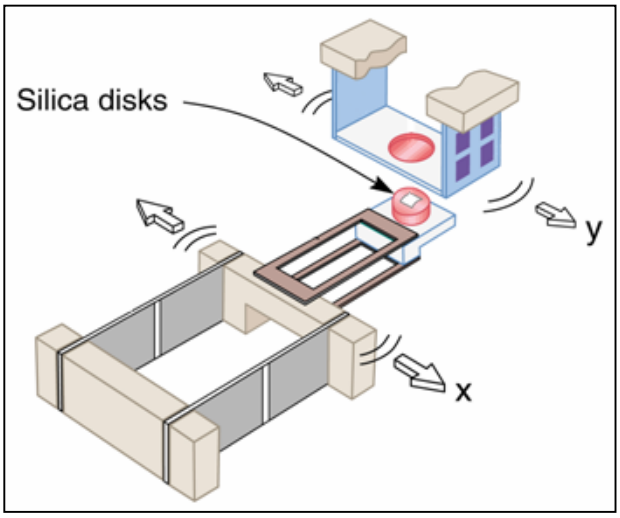

Figure 2.14 Friction force measurement in the surface force apparatus[21]

The lower surface is mounted on a bimorph slider that can shear surfaces. The bimorph slider is made from counter-aligned piezoelectric material. It can buckle back and forth when a triangle voltage is applied to it, shearing the surfaces against each other.

The upper surface is mounted on a cantilever spring with strain gauges, which can output a voltage corresponding to the displacement of the surface. Figure 2.15 shows a triangle wavevoltage applied to shear the surfaces and the corresponding output voltage detected by the strain gauge, from which we can calculate the friction force.

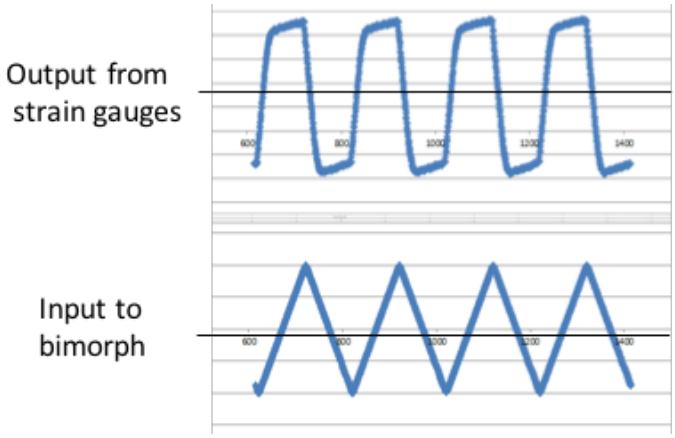

Figure 2.15 The triangle voltage input to the bimorph and the corresponding output signal generated by the strain gauges

We also have several friction devices with different spring stiffness. We can choose the suitable one according to the magnitude of friction is and the sensitivity that the measurement requires. For this polymer project, the friction force is very small. Therefore, we use the most compliant semiconductor friction device to detect the friction. Calibration is also needed before experiments. We hang small weights on the side of the friction device, applying a force to the cantilever spring and measure the corresponding output voltage, which can be translated into friction later. The calibration of the friction device used in this project can be found in the Appendix.

2.3 Results and discussion

To determine whether three types of lubricin mimetic polymers bind to the mica surfaces well, we used the SFA to perform normal force measurements to get the onset of interaction and “hardwall” thickness. Friction tests were performed at three different shearing frequencies. FECO were recorded to monitor the damage behavior to evaluate the wear protecting ability of mimLUBs.

Polymers were dissolved in DI water at a concentration of 3 mg/mL and shaken overnight using a spinner. The polymer solution was added between two surface mounted on the SFA for 1-hour incubation. Then we rinsed it 3 times with phosphate buffered saline (PBS) to remove free-floating polymer molecules. Normal force measurements and friction measurements were performed at multiple positions with different shearing velocities using the SFA.

We hypothesized that AB, ABA and random polymers might have different surface attachment to the mica surfaces and different lubrication abilities due to their different molecular structures, and that shearing velocity might affect the lubrication and damage behavior as well.

2.3.1 Friction coefficient

For mimLUB AB, five repeat experiments were carried out. In two of these experiments, the mica surfaces were not well prepared and the mica flakes were generated upon shearing caused immediate damage. Therefore, we did not include the results here. Figure 2.16 shows all the friction force vs. load plots, from which we calculated the friction coefficient (see inset table). Damage behavior was also recorded (friction measured when the damage occurred was marked with ○□△).

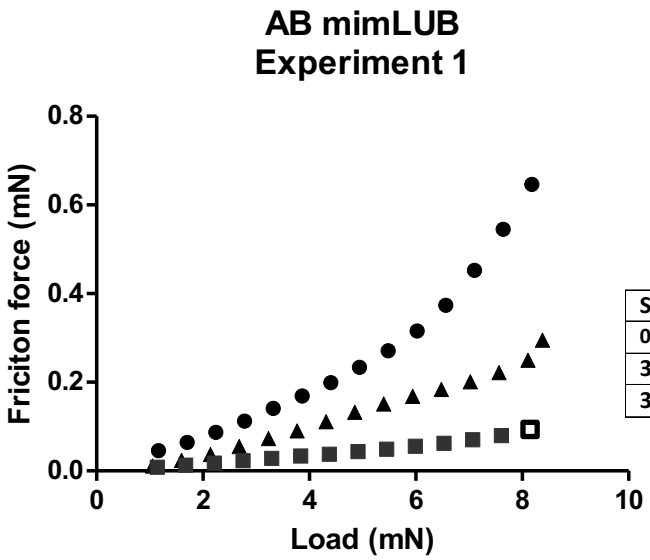

Shearing velocity	Friction coefficient
0.3µm/s	0.036
3 µm/s	0.011
30 µm/s	0.052-0.169

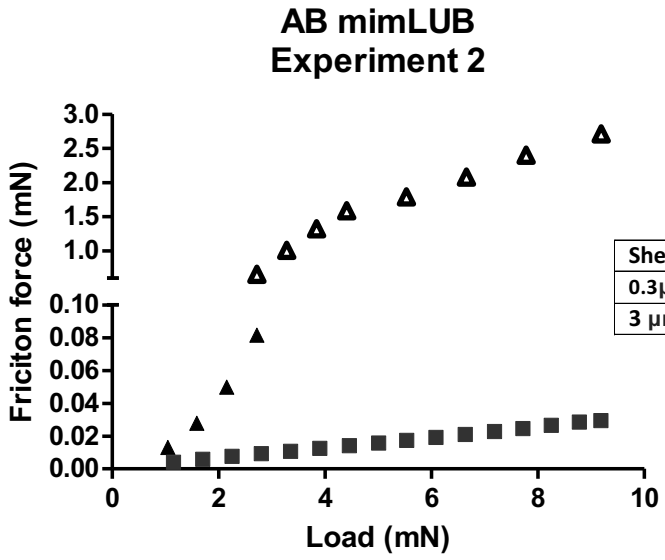

Shearing velocity	Friction coefficient
0.3µm/s	0.003
3 µm/s	0.04

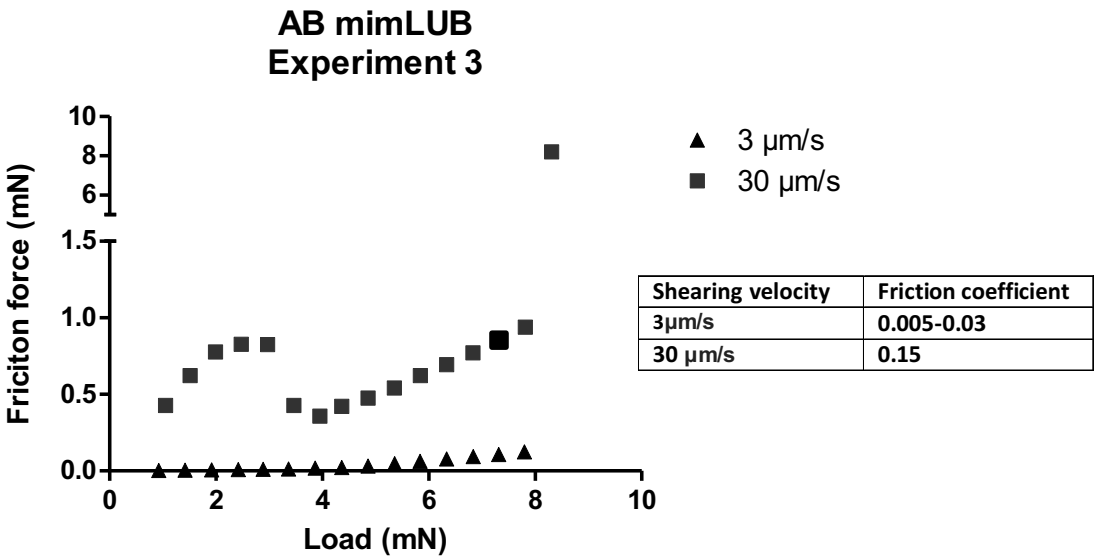

Figure 2.16 All friction versus load plots of AB mimLUB

While the friction coefficients of each shearing velocity measured in three experiments are not consistent, we note that all the friction coefficients measured are lower than that of shearing lubricin under the same condition regardless of shearing velocity (see Figure 2.17).

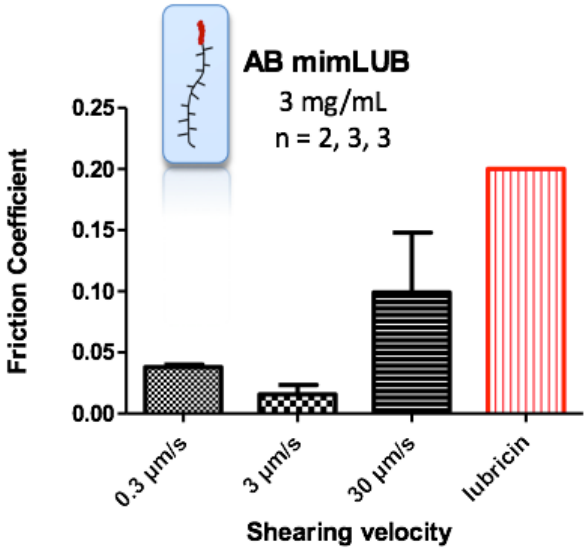

Figure 2.17 Average friction efficient of shearing AB mimLUB at various shearing velocities compared with lubricin (red bar)[20]

The red bar ($\mu = 0.20$) is the minimum friction coefficient measured when shearing lubricin in PBS at a shearing velocity of 1 µm/s[20]. The range is 0.20 to 0.60 (see Figure 2.2). The fact that the friction coefficients of all the experiments are lower than 0.20, plus damage only occurred twice among all the shearing tests prove that AB mimLUB has a good lubricating ability.

All friction versus load plots of shearing ABA mimLUB are shown in Figure 2.18.

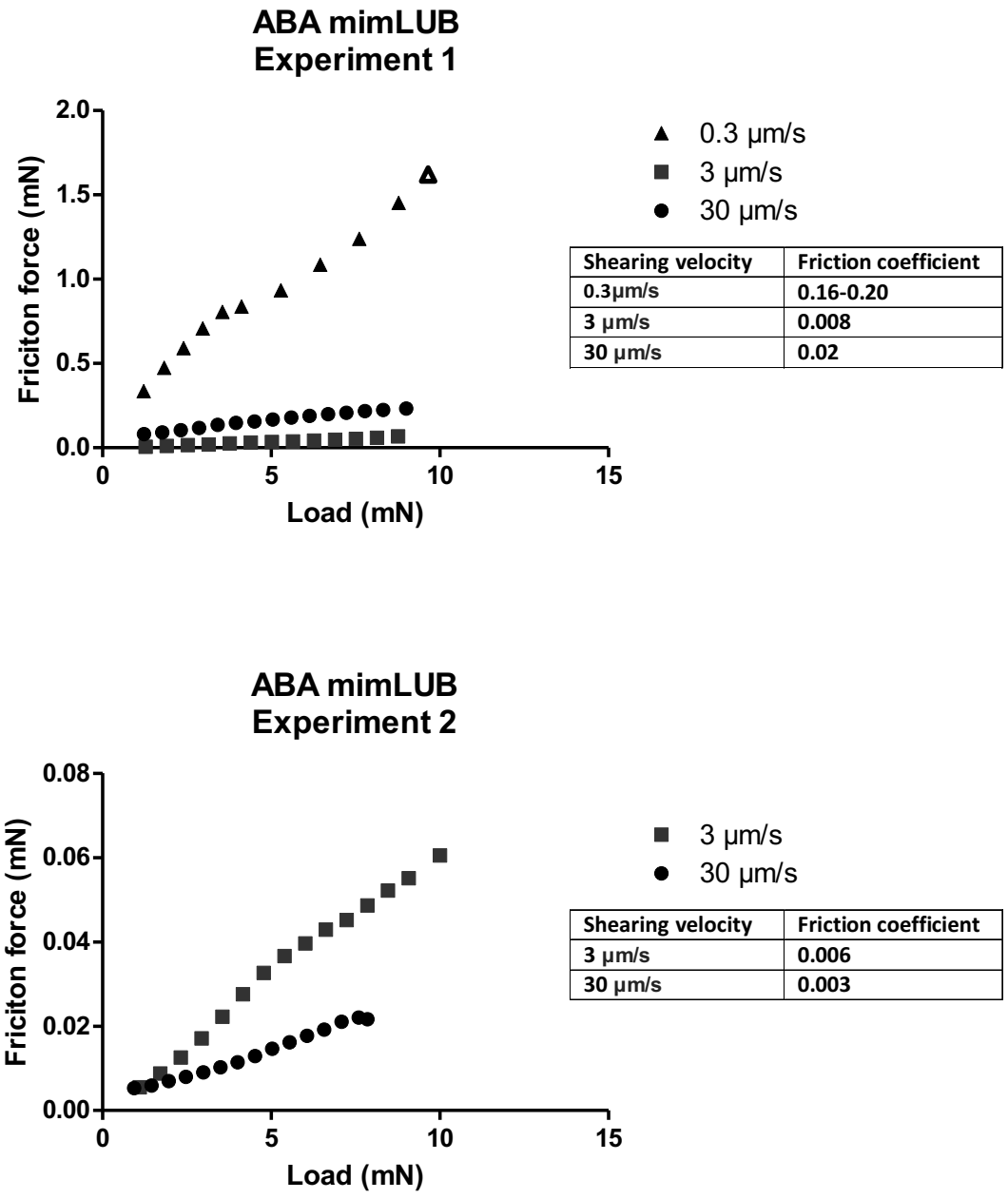

Figure 2.18 All friction versus load plots of ABA mimLUB

It is notable that apart from the friction test of 0.3 μm/s in Experiment 1 where damaged occurred at the end of the experiment, all the friction coefficients of shearing ABA are very low ($\mu < 0.02$) and damage did not occur. We note that ABA may have

an even better lubricating ability than AB. Figure 2.19 shows the average friction coefficient of each shearing velocity compared with shearing lubricin.

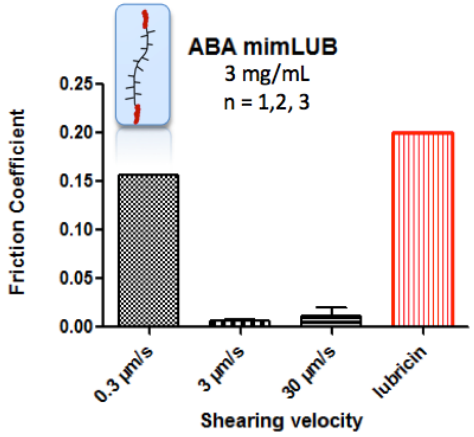

Figure 2.19 Average friction efficient of shearing ABA mimLUB at various shearing velocities compared with lubricin (red bar)[20]

As for Random mimLUB, in two repeat experiments, damage occurred immediatelyin all shearing tests and the friction coefficients are consistently high. We conclude that Random is a poor lubricant compared with AB and ABA.

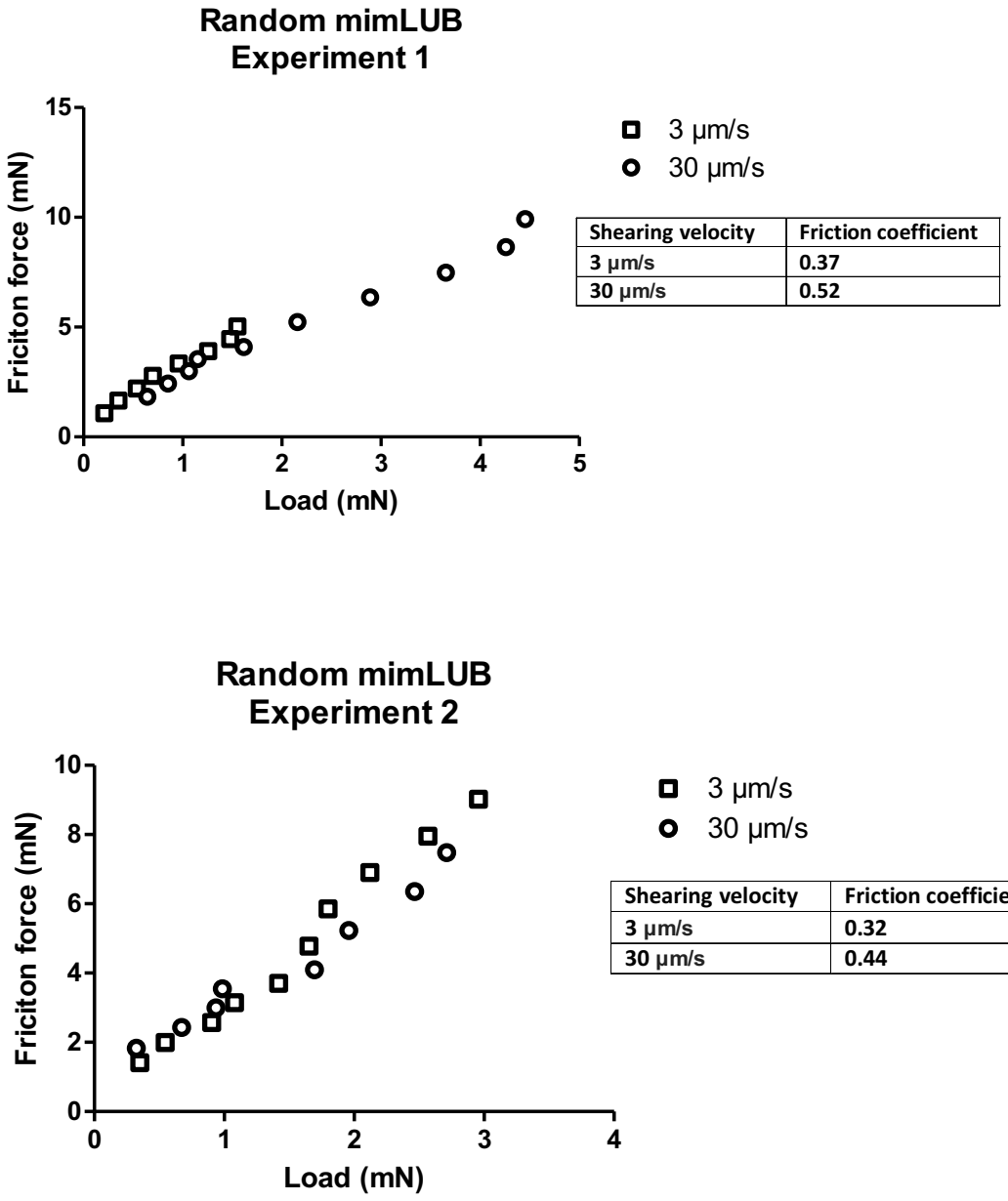

Figure 2.20 All friction versus load plots of Random mimLUB

Interestingly, the friction tests performed via a tribometer by Prof. Bonassar's group at Cornell give similar results (Figure 2.21 right). They used a different testing system where AB and Random mimLUB were sheared between cartilage and glass and the

load and pressure were both lower than us. Their sliding speed is 300 μm/s. We choose the results of our fastest velocity (i.e. 30 μm/s) for comparison (Figure 2.21 left).

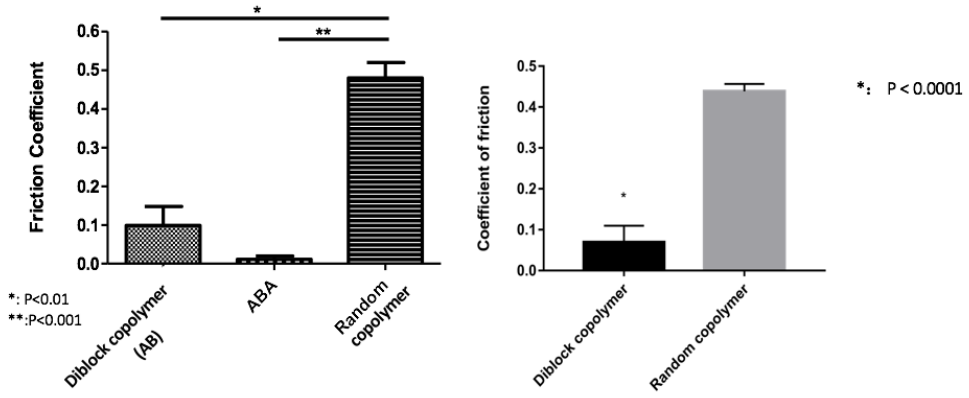

Figure 2.21 Average friction coefficient of various mimLUB tested via SFA (left) and tribometer (right)

The polymer concentration and incubation time are the same in these two methods. Although the surface, load, sliding speed are different, the friction coefficient turned out to be quite similar. AB diblock copolymer has a friction coefficient of 0.05-0.1 whereas the friction coefficient of Random mimLUB is approximately 0.45.

2.3.2 Damage behavior

Polymer	Number of total shearing tests done	Number of tests where damage occurred	Pressure before damage
AB	7	2	6.7 MPa, 4.6 MPa
ABA	5	1	7.4 MPa
Random	**4**	**4**	**Damage happened right away**

Table 2.1 Damage behavior of shearing three types of mimLUBs

Table 2.1 demonstrates the damage behavior of shearing AB, ABA and Random mimLUB. The results of all shearing velocities are grouped together. We note that shearing Random mimLUB caused damage immediately in all friction tests whereas AB and ABA have a much better wear protecting ability. Damage either did not occurred or occurred at relatively high pressure.

Based on the friction coefficient data and damage behavior, we conclude that AB and ABA are good lubricant whereas Random mimLUB has a poor lubricating ability.

2.3.3 Surface attachment

In Chapter 1 we introduce key factors of good lubrication: hydrophilic bottle-brush architecture and strong surface attachment. AB, ABA and Random have the same brush structure. So we hypothesize that the ability to attach to the surfaces varies among them and the bad lubricating ability of Random mimLUB may be due to its poor surface attachment.

To characterize the surface attachment of three types of mimLUBs, normal force measurements were performed to determine the onset of interaction and the “hardwall” thickness. The results are shown in Figure 2.22.

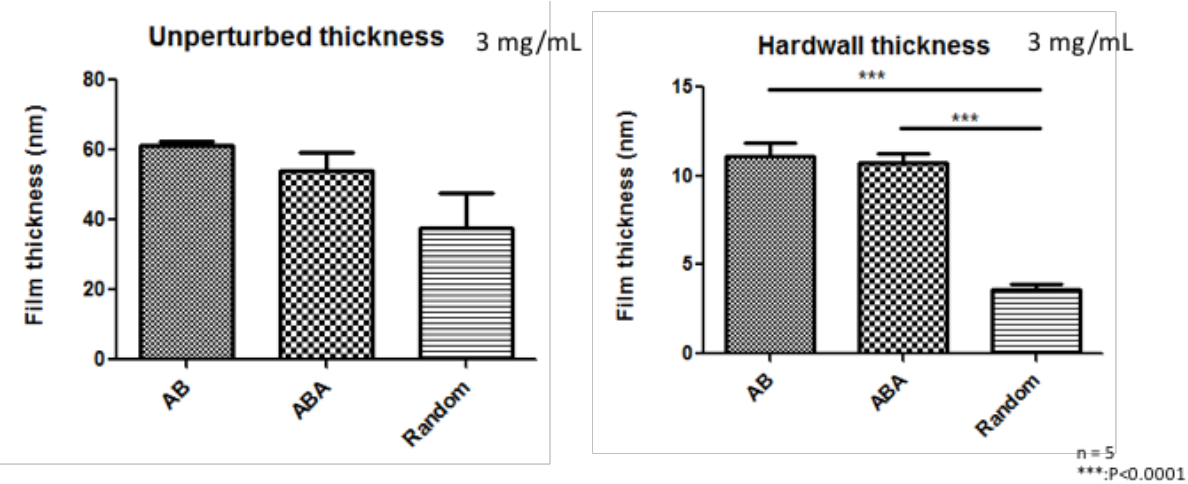

Figure 2.22 Unperturbed thickness and hardwall thickness of 3 mg/mL AB, ABA and Random mimLUB incubated for 1 hour

Given that the hydrodynamic size of Random mimLUB is the smallest among three mimLUBs, t is not surprising that the unperturbed film thickness of Random mimLUB is slightly smaller (not statistically significant) than AB and ABA. However, the hardwall thickness of Random mimLUB is significantly smaller than the other two mimLUBs. Figure 2.23 illustrates one possible interpretation of the results:

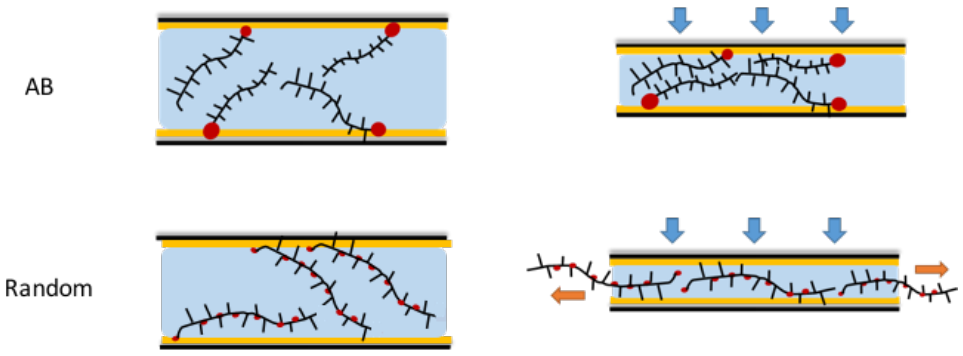

Figure 2.23 Schematics of possible surface attachment of AB and Random mimLUB at low and high load/pressure

AB and ABA have terminal binding units where the positively charged binding groups gather together to ensure a strong attachment to the surface. However, the binding groups in Random mimLUBs are distributed randomly and sparsely. Therefore, the polymers bind to the surfaces so weakly that once sheared or compressed they tend to be squeezed out, which explains the significantly lower hardwall thickness of Random mimLUB compared with AB and ABA.

CHAPTER 3

CONFORMATIONAL STUDY OF LUBRICIN-MIMETIC POLYMERS

3.1 Introduction

3.1.1 Conformation of lubricin on surfaces

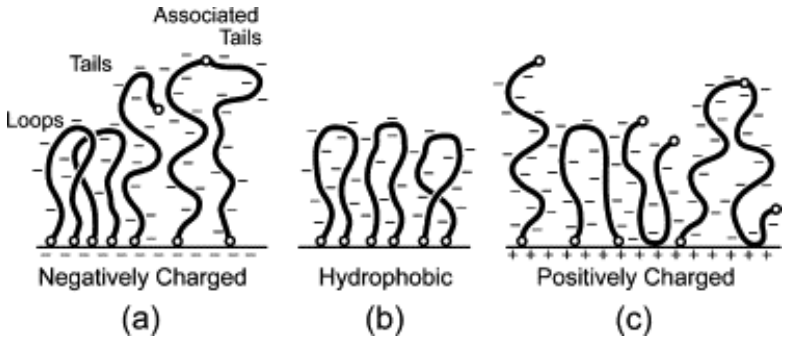

Figure 3.1 Proposed conformation of lubricin on (a) mica, (b) alkanethiol, and (c) aminothiol[20]

Zappone et al. proposed that lubricin tends to adopt both loop and tail conformation based on their normal force measurement[20]. The dominant conformation on mica is loop-like. The average height of the loop is 60 nm, which is equal to 30% of the stretched molecular length measured via bridging experiment. The onset of interaction is measured between two lubricin-coated mica. Shorter range of onset of interaction is 130 nm, corresponding to two-layer loop-like lubricin. Longer range of onset of interaction is also found to match the tail-like conformation but it disappears after rinsing or repeating the force run at the same position. It is because the tail-like lubricin is more weakly bound to the surface than loops.

3.1.2 Bridging experiment

When studying lubricin on mica surfaces, Zappone et al. proposed an interesting force measurement between one lubricin-coated surface and one bare mica surface[20]. First, they incubated lubricin solution on both mica surfaces. Then they rinsed with PBS and replaced the top surface with a new bare mica surface. The surfaces were brought closer and they waited 10-120 min for the polymer to bridge to the top surface. The in-run showed a very weak attractive force due to the attraction between the positively charged binding domain of lubricin and negatively charged mica. On retracting the surface (out-run), an adhesion force of -1.5 mN/m was observed. The adhesion is caused by lubricin molecules binding onto the bare mica surface. Importantly, the maximum bridging distance between two surfaces is considered to be the extended length of the lubricin molecule.

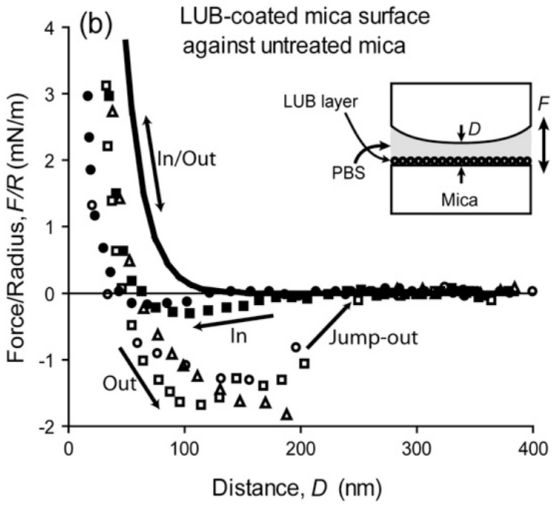

Figure 3.2 Force run curves between a lubricin-coated surface and an uncoated mica surface in PBS[20]

Bridging experiment is extremely helpful to measure the extended length of both lubricin and lubricin-mimetic polymers. One important prerequisite is that the lubricin-mimetic polymer must have binding groups at both ends of the molecule in order to bridge between two surfaces.

3.2 Materials and Methods

3.2.1 Bridging experiment

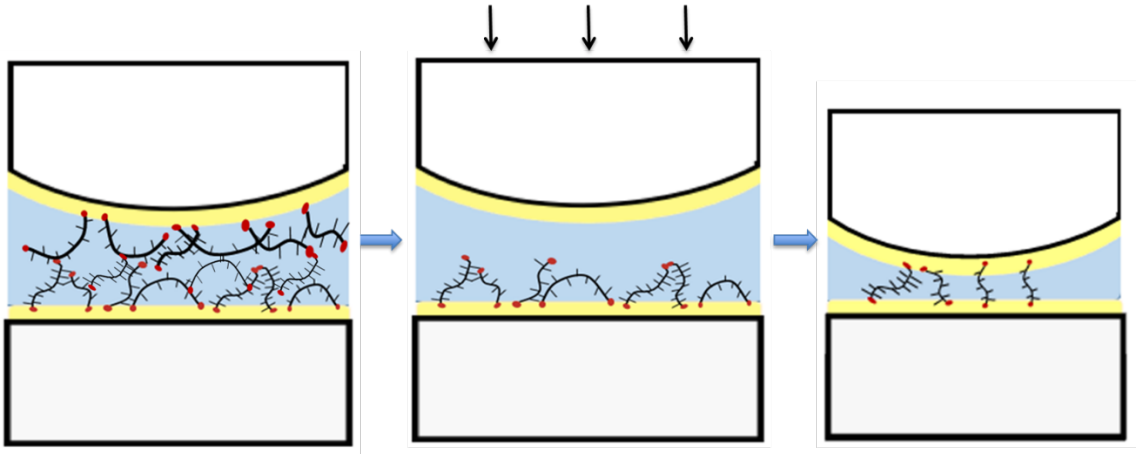

Figure.3.3 Schematics showing the procedure of bridging experiment

The bridging experiment was performed following the protocol below:

(1) Prepare three surfaces with the same mica thickness

(2) Incubate with 3 mg/ml ABA mimLUB for 1 hour

(3) Rinse with PBS 5 times to fully get rid of the free-floating polymers

(4) Replace the top surface with a bare mica surface

(5) Bring surfaces closer (in-run) and wait 40 min for bridging

(6) Separate the surfaces (out-run)

3.2.2 Surface mount with piezoelectric tube

In the previous chapter, three different ways of moving the bottom surface to control the distance between two surfaces are introduced: coarse micrometer, medium micrometer and motor-driven micrometer. There is another approach which moves the upper surface to control the distance. The upper surface is supported in a mount that has a piezoelectric tube. By changing the voltage across the inside and outside walls of the tube, it can reach a total range of movement of 1 μm and the accuracy can be greater than 1 Å. Another advantage is that we can change the voltage very slowly so that the distance between two surfaces can increase or decrease much more slowly than using the motor-driven micrometer.

In order to precisely measure the onset of interaction and the "hardwall" thickness, we chose to use the piezoelectric mount to carry on the normal force measurement in this chapter. In the case where the bridging was very strong and the deformation range of piezoelectric mount was not enough to let the surfaces detached from each other, the motor was used with the slowest speed. We also used a more compliant spring. The calibration of the cantilever spring can be found in the Appendix.

There are two different approaches to change the voltage across the inner and outer walls of the piezoelectric tube.

3.3 Results and discussion

3.3.1 Bridging experiment

The normal force measurement of the bridging experiment is shown in the Figure 3.6. During the in-run, the top surface is brought down slowly. Since the end of the ABA mimLUB is positively charged quaternary amine group, when it is approaching negatively charged mica surface, we expect an attraction force. However, our force curve does not show a negative force, mainly because the attractive force is too weak to be detected by our device. It is not likely that all the ABA tail ends absorb onto the mica surface at the same time to create a large attraction.

When the surface distance is smaller than 50 nm, the positive force takes over. The repulsion is caused by steric-entropic interaction. After the onset of interaction (i.e. at smaller separation distance), bridging bond is also formed due to the opening of some of the loops that are originally reside only on the bottom surface and bridging to the upper surface.

On separation of the surfaces, firstly the steric repulsion dominates. However, after 40 min bridging, there are much more bridges than on approach, making the attractive force larger. As we separate the surface, the repulsive force decreases and the attractive force increases. At some point, the attractive force takes over and the situation now is like stretching the spring. The bridges are stretched and some start to detach from the surface. The separation distance where attraction force reaches the climax corresponds to the maximum length of a stretched bridge before breaking.

When the surfaces are brought farther than this “extended length”, more and more bridges are broken and the attractive force disappears quickly.

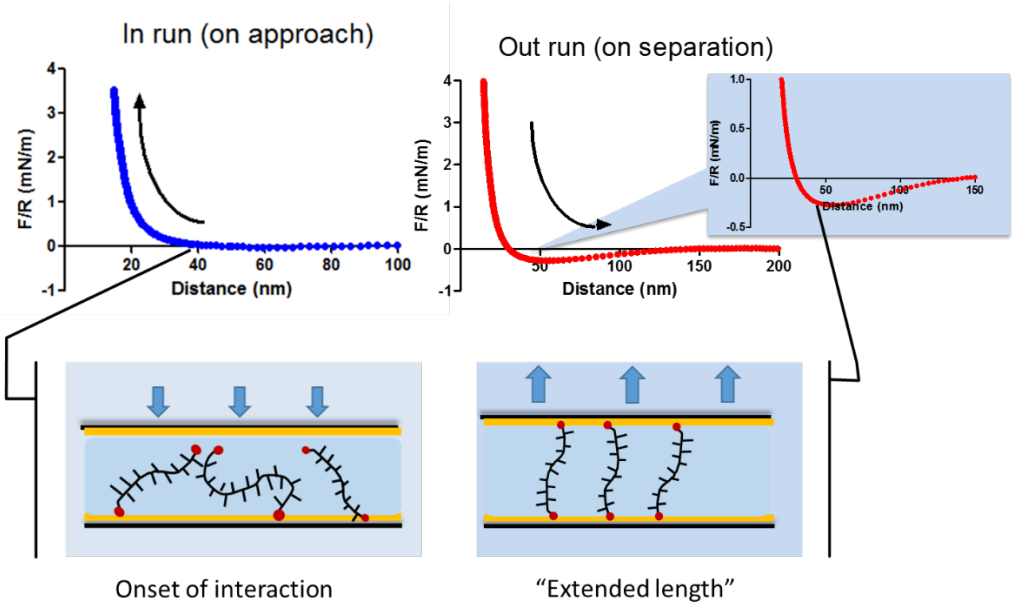

Figure 3.6 Normal force measurement of ABA mimLUB at 3 mg/ml between mica surfaces

3.3.2 Conformation of mimLUB on mica surface

We compare the extended length of ABA mimLUB with the onset of interaction of ABA against the bare mica (Figure 2.7). The fact that the extended length is significantly larger proves that the conformation of the ABA mimLUB on mica before compressing and shearing is not exactly “tail-like”.

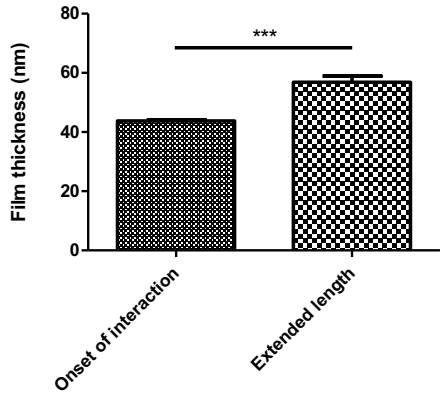

Figure 3.7 Onset of interaction of ABA-mica and the extended length of ABA

Given the fact that the extended length of ABA mimLUB measured via bridging experiment is 56.81 ± 2.11 nm, plus previous normal force run measurement of ABA-ABA indicates the onset of interaction is 54.00 ± 5.132 nm, we exclude the possibility that ABA adopts the tail-like conformation because onset of interaction should be ~100 nm instead (Figure 2.8 left). We proposed that ABA mimLUB mainly adopts "bent" conformation as shown in the middle of Figure 3.13. If ABAs form loops, the height of the loop is less than 50% of the extended length. The film thickness of double layers of loops once interacted with each other is smaller than 56.81 nm. But it is also a possible conformation since our normal force runs measure the initial interaction from both sides, created by the tallest molecules on both sides. Shorter molecules in loop conformation would interact with either bent or loop molecule later. Therefore, most likely, the conformation of ABA mimLUB on mica surface before compressing and shearing is a combination of bent and loop structure, which is similar to lubricin (Figure 3.8).

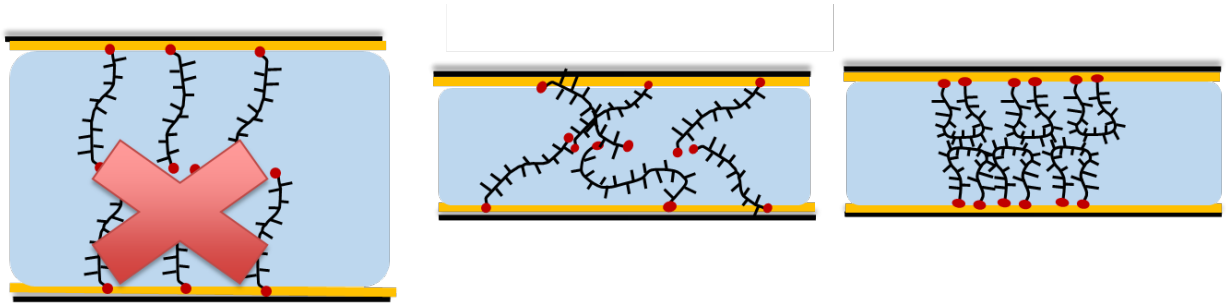

Figure 3.8 Schematics of the proposed conformation of ABA mimLUB on mica surface

The extended length of AB mimLUB remains unknown because it does not have two binding groups on both ends to bridge between two surfaces. However, given the fact that the lubricating domain is the same in AB and ABA, we believe that the extended length of AB is similar to AB. Other characterization techniques are required to accurately determine the contour length of AB in order to understand its conformation on mica surfaces.

As for the conformation under high load, we hypothesize that both AB and ABA are lying down to form a monolayer on each surface Since we do not have AFM data, we did a theoretical calculation of the length of the PEG side chain. PEG400 (n=9) has a contour length of 2.52 nm based on the PEG unit length of 0.28 nm in water[24]. Given the fact that both AB and ABA have a hardwall value of ~11 nm. We propose that the mimLUBs tend to "lie down" to bilayer as shown in Figure 3.9.

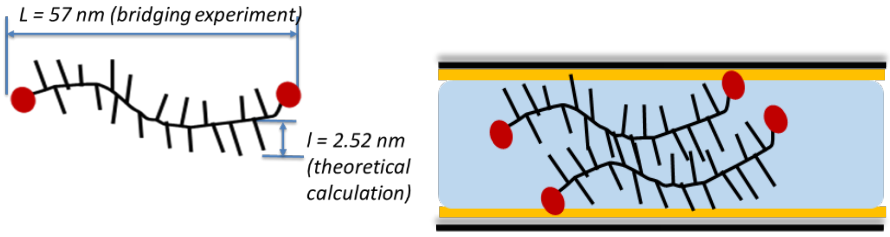

Figure 3.9 Extended length of ABA mimLUB and proposed conformation of ABA under high loads.

3.3.3 Dependency of the film thickness on polymer concentration

Accurate normal force measurements were also performed to further investigate whether the polymer concentration and incubation time might have an impact on the surface attachment and binding density.

Both AB and ABA mimLUBs at three different concentrations (i.e. 0.3 mg/mL, 1.5 mg/mL, 3 mg/mL), were incubated for 1 hour. Normal force measurement was performed by SFA with piezoelectric mount and a more compliant spring to achieve higher accuracy. The results are shown in Figure 3.10.

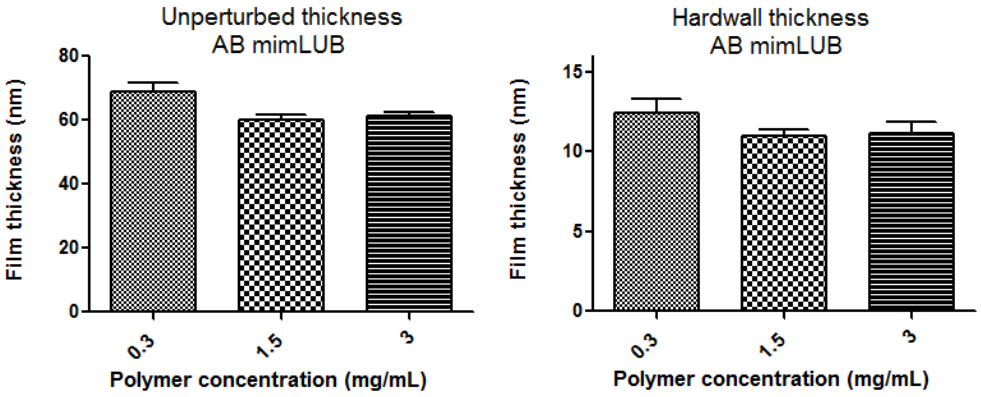

Figure 3.10 Unperturbed film thickness and hardwall thickness of AB mimLUB at different concentrations after incubated 1 hour between mica surfaces

From Figure 3.10 we note that neither the unperturbed thickness nor the hardwall thickness changes over three different concentrations. The values are ~60 nm and ~11 nm respectively. The normal force measurement was performed at 5 different positions for each concentration. The fact that all the measurements are very consistent proves that AB mimLUB forms a uniform layer which covers the mica surface completely. This uniform layer is formed at or below 0.3 mg/mL thus higher concentrations do not increase the film thickness. We hypothesized that the friction should be similar among these concentrations but the experiments were not done yet.

Figure 3.11 shows the results of the concentration dependency of AB mimLUB measured by a tribometer. This work is done by Bonassar's group at Cornell. The system they used is different from us. They use a higher sliding speed (300 μm/s) and a lower load and the mimLUB was sheared between cartilage-glass surfaces. The results indicate that below 1 mg/ml, higher concentration leads to lower COF whereas

above 1 mg/ml it reaches a plateau and the COF remains constant regardless of the concentration.

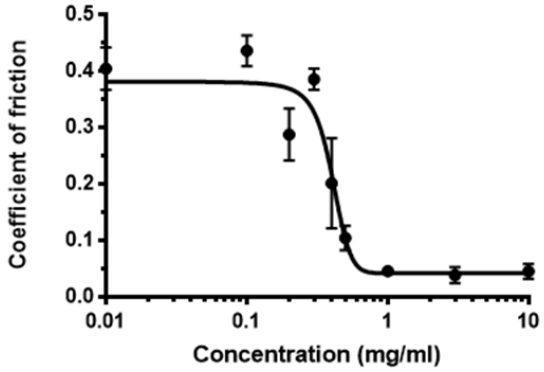

Figure 3.11 Friction of coefficient of AB mimLUB at different concentrations measured with tribometer (data obtained from Elizabeth Feeney, Bonassar's group, manuscript in preparation)

There should be a similar trend for our system but the threshold value is smaller than 0.3 mg/ml. Further study on the friction and film thickness at concentrations lowerthan 0.3 mg/ml is needed.

Similar results for ABA mimLUB are shown in Figure 3.12. The onset of interaction of ABA is slightly smaller than that of AB but it also does not change a lot among different concentrations.

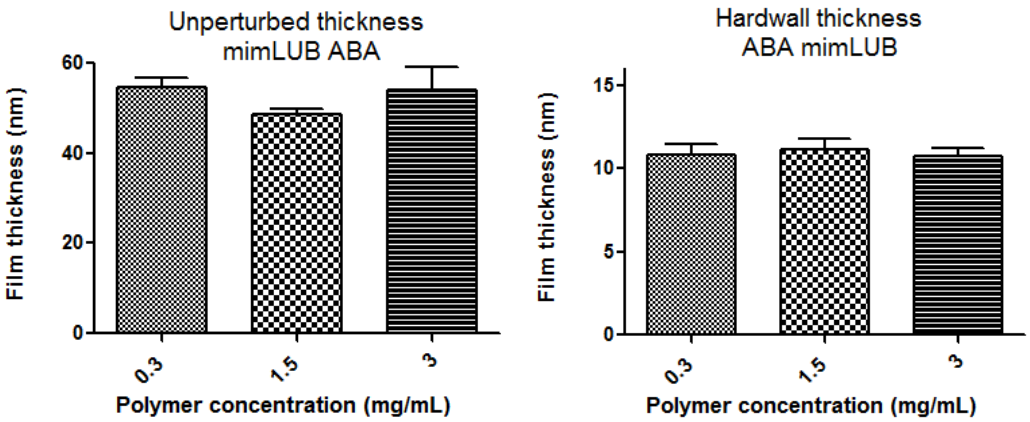

Figure 3.12 Unperturbed film thickness and hardwall thickness of ABA mimLUB at different concentrations after incubated 1 hour between mica surfaces, n = 5

3.3.4 Dependency of the film thickness on incubation time

The film thickness of AB mimLUB at 3 mg/ml with different incubation times is also measured. While there is no significant difference between 1-hour and 3-hour incubation, AB mimLUB incubated for 3 min has a significant smaller thickness under compression. We note that among 5 different positions, two positions show similar thickness to normal condition (i.e. 1-hour incubation) whereas the thickness at the other three positions is close to zero. It indicates that after 3-min incubation, a uniform polymer layer which covers the whole surface was not formed.

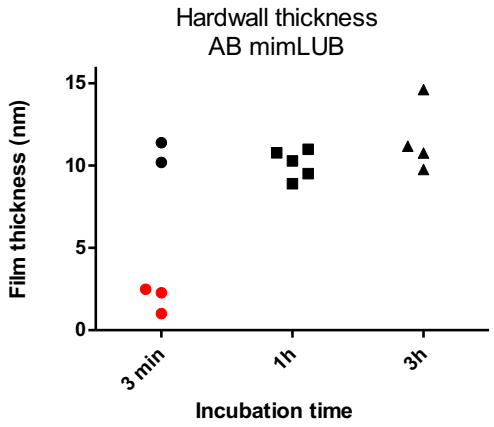

Figure 3.13 Hardwall thickness of AB mimLUB at 3 mg/ml with different incubation time, n = 5

Similar results were measured by the tribometer. From Figure 3.14, we note that at least 30-min incubation time is needed to ensure a good lubrication (low COF). In our case the least required incubation time may vary but we can get the result by measuring the friction of mimLUBs with different incubation time by SFA. However, all of our friction experiments, we incubated for 1 hour, which is a sufficient time to ensure the formation of a uniform, strongly-attached polymer film.

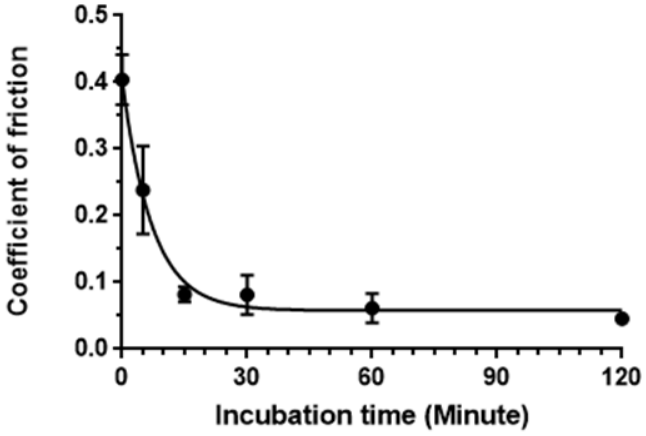

Figure 3.14 Friction of coefficient of AB mimLUB with different incubation time measured with tribometer (data obtained from Elizabeth Feeney, Bonassar's group, manuscript in preparation)

CONCLUSION AND FUTURE WORK

Three types of lubricin-mimetic polymers were synthesized and we characterized their surface attachment, tribological properties and wear protection. AB and ABA mimLUB have a lower friction coefficient compared with lubricin sheared under the same condition. They also exhibit a strong surface attachment and good wear protection. However, Random mimLUB caused surface damage once being sheared. Its poor lubricating ability might be due to weak surface attachment caused by the difference in molecular structures from the other two mimLUBs.

Bridging experiments were carried out to measure the extended molecular length of ABA and determine the conformation on surfaces. We propose that ABA adopt a combination of bent and loop-like conformation on mica surface before compressing and shearing. At high load and pressure, both AB and ABA molecules tend to lie down to form a double layer. To better understand the conformation of mimLUB, more accurate coutour length measurement is needed.

Further normal force measurements indicate that incubation time is a key parameter to reach high binding density and ensure good lubrication. Different concentrations (0.3, 1.5, 3 mg/mL) of mimLUB show similar surface attachment. The least required concentration for forming a film that covers the surface uniformly might be even lower than 0.3 mg/mL and requires future investigation.

AB and ABA mimLUB are considered to be good lubricants. Further investigation on the interaction between mimLUBs and synovial fluid components (e.g. fibronectin,

collagen and hyaluronic acid) and in vivo studies are required to make mimLUB a potential alternative to lubricin.

APPENDIX

1. Friction device calibration

Force	Actual Voltage
mN	V
9.803	0.008133333
11.3018787	0.009525
19.606	0.016491667
29.409	0.024516667
39.212	0.032666667

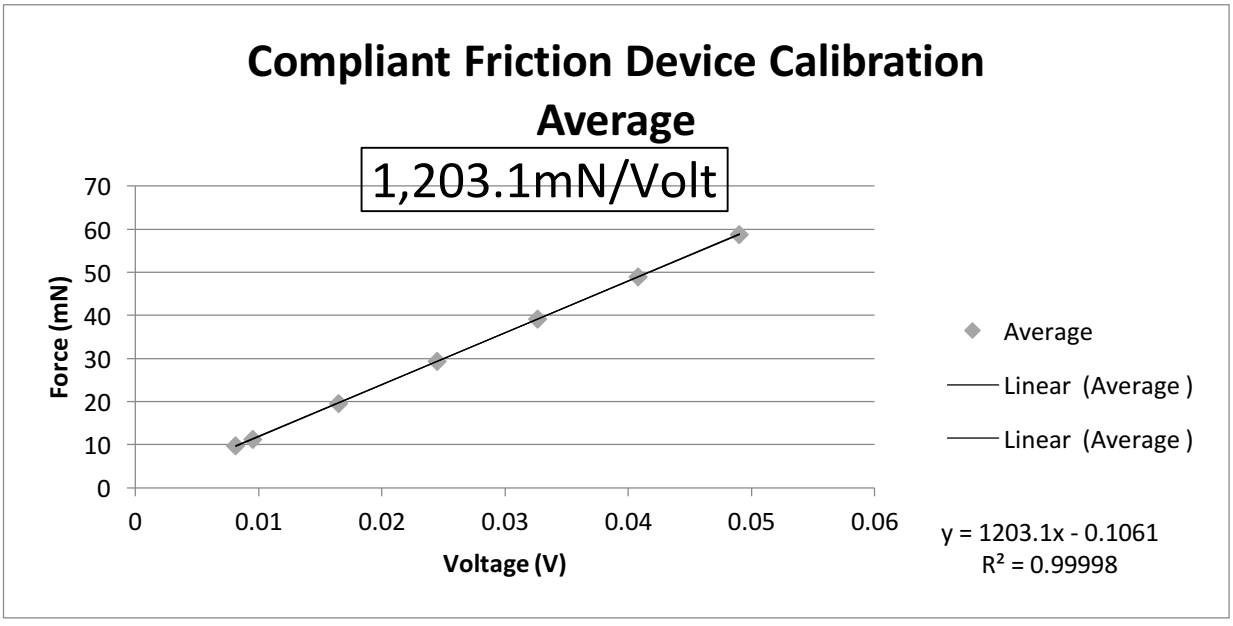

2. Spring calibration

mass (Kg)	displacement (m)	force (N)
0	0	0
0.001153	0.000055	0.011298
0.002153	0.0001075	0.021098
0.003153	0.000155	0.030898
0.004153	0.0002225	0.040698
0.005153	0.00027	0.050498
0.006153	0.000345	0.060298

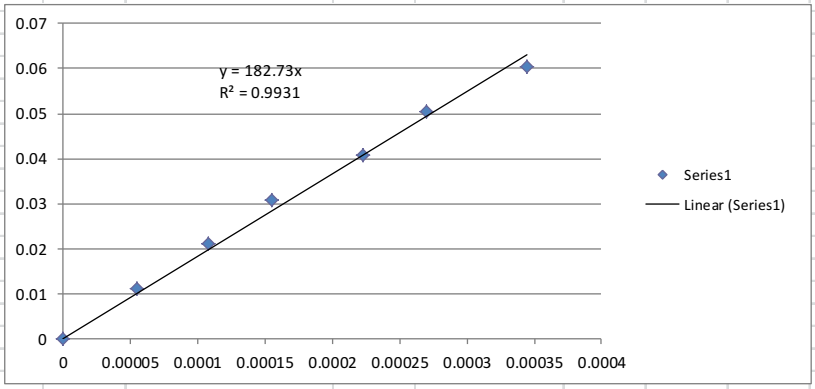

First measurement K (mN/m)	Second measurement K (mN/m)	
182730	186880	184805

mass (Kg)	displacement (m)	force (N)
0	0	0
0.001153	0.00006	0.011298
0.002153	0.000115	0.021098
0.003153	0.0001675	0.030898
0.004153	0.00022	0.040698
0.005153	0.0002675	0.050498
0.006153	0.0003225	0.060298

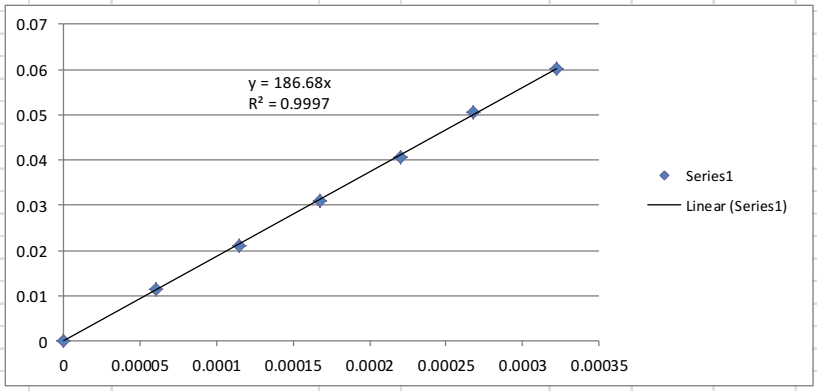

REFERENCES

1. Morrell, K. C., Hodge, W. A., Krebs, D. E. & Mann, R. W. Corroboration of in vivo cartilage pressures with implications for synovial joint tribology and osteoarthritis causation. *Proc. Natl. Acad. Sci. U. S. A.* **102,** 14819–14824 (2005).

2. Shakoor, N. & Loeser, R. Osteoarthritis. *Sci. aging knowlege Environ.* (2004).

3. Kuettner, K. *articular cartilage and osteoarthritis*. (Lippincott Williams & Wilkins, 1992).

4. Musumeci, G. The role of lubricin in normal and pathological joint tissue: a contemporary review. *OA Anat.* **1,** 2 (2013).

5. Eguiluz, R. C. A. *et al.* Fibronectin mediates enhanced wear protection of lubricin during shear. (2015). doi:10.1021/acs.biomac.5b00810

6. Flannery, C. R. *et al.* Prevention of cartilage degeneration in a rat model of osteoarthritis by intraarticular treatment with recombinant lubricin. *Arthritis Rheum.* **60,** 840–847 (2009).

7. Matter, S. Biomimetic lubrication. (2012). doi:10.1039/c1sm06335a

8. Estrella, R. P., Whitelock, J. M., Packer, N. H. & Karlsson, N. G. The glycosylation of human synovial lubricin: implications for its role in inflammation. *Biochem. J.* **429,** 359–367 (2010).

9. Raviv, U. *et al.* Lubrication by charged polymers. *Nature* **425,** 163–165 (2003).

10. Jones, A. R. C. *et al.* Binding and localization of recombinant lubricin to

articular cartilage surfaces. *J. Orthop. Res.* **25,** 283–292 (2007).

11. Zappone, B., Greene, G. W., Oroudjev, E., Jay, G. D. & Israelachvili, J. N. Molecular aspects of boundary lubrication by human lubricin: effect of disulfide bonds and enzymatic digestion. *Langmuir* **24,** 1495–1508 (2008).

12. Banquy, X., Burdyńska, J., Lee, D. W., Matyjaszewski, K. & Israelachvili, J. Bioinspired bottle-brush polymer exhibits low friction and Amontons-like behavior. *J. Am. Chem. Soc.* **136,** 6199–6202 (2014).

13. Samaroo, K. J., Tan, M., Putnam, D. & Bonassar, L. J. Binding and lubrication of biomimetic boundary lubricants on articular cartilage. *J. Orthop. Res.* **35,** 548–557 (2017).

14. Eguiluz, R. A. E. *et al.* Synergistic interactions of a synthetic lubricin mimetic with fibronectin for enhanced wear protection. *Front. Bioeng. Biotechnol.* **5,** 36 (2017).

15. Andresen Eguiluz, R. C. *et al.* Fibronectin mediates enhanced wear protection of lubricin during shear. *Biomacromolecules* **16,** 2884–2894 (2015).

16. Radin, E. L., Swann, D. A. & Weisser, P. A. Separation of a hyaluronate-free lubricating fraction from synovial fluid. *Nature* **228,** 377–378 (1970).

17. Swann, D. A., Hendren, R. B., Radin, E. L. & Sotman, S. L. The lubricating activity of synovial fluid glycoproteins. *Arthritis Rheumatol.* **24,** 22–30 (1981).

18. Bhushan, B., Israelachvili, J. N. & Landman, U. Nanotribology: friction, wear and. *Nature* **374,** 13 (1995).

19. Kappl, M. *Surface and interfacial forces*. (John Wiley & Sons, 2009).

20. Zappone, B., Ruths, M., Greene, G. W., Jay, G. D. & Israelachvili, J. N. Adsorption, Lubrication, and Wear of Lubricin on Model Surfaces: Polymer Brush-Like Behavior of a Glycoprotein. *Biophys. J.* **92,** 1693–1708 (2007).

21. Israelachvili, J. N. *User's manual for SFA3 and SFA2000 with attachments*. (2009).

22. https://en.wikipedia.org/wiki/Newton%27s_rings.

23. Israelachvili, J. *et al.* Recent advances in the surface forces apparatus (SFA) technique. *Reports Prog. Phys.* **73,** 36601 (2010).

24. Ma, Z. *et al.* PEG linkers and properties. (2014). doi:10.1371/journal.pone.0112292.t001